

Optomechanical Micro-Macro Entanglement

R. Ghobadi,^{1,*} S. Kumar,¹ B. Pepper,² D. Bouwmeester,^{2,3} A. I. Lvovsky,^{1,4} and C. Simon¹
¹*Institute for Quantum Science and Technology, Department of Physics and Astronomy, University of Calgary,
 Calgary T2 N 1N4, Alberta, Canada*

²*Department of Physics, University of California, Santa Barbara, California 93106, USA*

³*Huygens Laboratory, Leiden University, P.O. Box 9504, 2300 RA Leiden, Netherlands*

⁴*Russian Quantum Center, 100 Novaya Street, Skolkovo, Moscow 143025, Russia*

(Received 30 August 2013; published 27 February 2014)

We propose to create and detect optomechanical entanglement by storing one component of an entangled state of light in a mechanical resonator and then retrieving it. Using micro-macro entanglement of light as recently demonstrated experimentally, one can then create optomechanical entangled states where the components of the superposition are macroscopically different. We apply this general approach to two-mode squeezed states where one mode has undergone a large displacement. Based on an analysis of the relevant experimental imperfections, the scheme appears feasible with current technology.

DOI: 10.1103/PhysRevLett.112.080503

PACS numbers: 03.67.Bg, 03.65.Ta, 42.50.Wk, 42.50.Xa

Vigorous efforts are currently being undertaken to bring quantum effects such as superposition and entanglement to the macroscopic level [1–9]. One prominent goal in this context is the creation of entanglement between a microscopic and a macroscopic system [2–9], following Schrödinger’s famous thought experiment that involved a decaying nucleus and a cat [10]. In optomechanical systems the quantum regime has recently been reached [11–14], but optomechanical entanglement has not yet been demonstrated. In a certain sense any entanglement of an optomechanical system can be seen as micro-macro entanglement, because the mechanical system always involves billions of atoms. However, for many proposals [15–17] the different components of the entangled state only differ by (of order) a single phonon.

Here we show how to create optomechanical micro-macro entanglement in a stronger sense by combining two key ideas. First, we propose a convenient method for both creating and detecting optomechanical entanglement, based on mapping one component of an entangled state of light onto the mechanical resonator and then retrieving it [18,19]. Demonstrating entanglement for the retrieved light then demonstrates the existence of optomechanical entanglement in the intermediate state. Second, we show that this approach makes it possible to create optomechanical “cat states” where there is a macroscopic difference for a physical observable between the different components of the superposition, based on recent work demonstrating micro-macro entanglement of light [3–6]. The physical observable in our case is the variance of the phonon number. Our proposal is thus different from Ref. [20], which aim to create superposition states of mechanical systems with a large separation in position.

We propose to first create purely optical micro-macro entanglement by amplification of one component of an

initial microscopic entangled state [3–8], and to then convert the photons in the amplified component into phonons. The entanglement can be verified by reconverting the phonons into photons and using the deamplification and detection techniques of Refs. [3–6]. Deamplification is advantageous in practice compared to trying to verify micro-macro entanglement by direct detection, which requires extremely high measurement precision [21].

The general approach described above can be applied to different micro-macro entangled states [3–8]. We illustrate it by introducing two-mode squeezed states where one mode has undergone a large displacement. We propose to use displacement as the amplification process because it creates states that are comparatively robust under photon loss [3,4,6]. Displaced two-mode squeezed states furthermore have the interesting property that the degree of entanglement and the degree of macroscopicity can be varied almost independently by choosing the amount of squeezing and the size of the displacement. Moreover, these states are Gaussian, making it possible to quantify their entanglement exactly even in the presence of imperfections. See the Supplemental Material [22] for the application of our approach to displaced single-photon entanglement [3,4,6].

We start by creating a two-mode squeezed state $|\psi_0\rangle = \sqrt{1-t^2} \sum_{n=0}^{\infty} t^n |n\rangle_A |n\rangle_C$ with $t = \tanh(r)$ where r is the squeezing strength. For moderate r only the first few terms contribute significantly. For example, for $r = 0.5$ (or 4.3 dB of squeezing) the probabilities for the first terms are $p_{00} = 0.786$, $p_{11} = 0.168$, $p_{22} = 0.036$, and the total weight of the remaining terms is only 0.001. We denote the optical modes A and C , reserving the label B for the mechanical oscillator. We apply the displacement operator $D(\alpha) = e^{\alpha a^\dagger - \alpha^* a}$ in mode A , generating the state

$$|\psi_D\rangle = \sqrt{1-t^2} \sum_{n=0}^{\infty} t^n (D(\alpha)|n\rangle)_A |n\rangle_C. \quad (1)$$

The displacement can be implemented by interference with a strong coherent beam [3,4,6,23,24], see Fig. 1. A displaced Fock state $D(\alpha)|n\rangle$ has a photon number variance $(2n+1)|\alpha|^2$. For moderate r and large α the state (1) is thus a superposition of a small number of relevant components that have macroscopically distinct photon number variances. Increasing the displacement α increases the macroscopicity of the superposition. On the other hand, increasing the squeezing parameter r increases the entanglement of the state, in particular the number of components that contribute significantly. Here we focus on the moderate squeezing regime with only a few components, which is also the easiest regime to achieve experimentally.

The displaced mode A of the two-mode squeezed state is now fed into a cavity and stored onto the mechanical mode B using the optomechanical coupling between the cavity field and the mechanical mode [18,19], see Fig. 1. The basic optomechanical Hamiltonian is $H = \hbar\Delta a^\dagger a + \hbar\omega_m b^\dagger b + \hbar g_0 a^\dagger a (b + b^\dagger)$, where $\Delta = \omega_c - \omega_L$ is the detuning between the cavity resonance and the frequency of the control beam (see below), a is the annihilation operator for the cavity mode, ω_m is the mechanical

resonance frequency, b is the mechanical mode annihilation operator, g_0 is the bare optomechanical coupling, and the Hamiltonian is written in the rotating frame with respect to the frequency of the control beam. If the control beam is red detuned by ω_m with respect to the cavity resonance (and if $\omega_m \gg \kappa$, the resolved-sideband regime), one obtains the effective beam splitter Hamiltonian $H_{\text{eff}} = g(a^\dagger b + ab^\dagger)$, where g is proportional to g_0 and to the amplitude of the control beam [13,25]. The resulting equations of motion are $\dot{a} = -\kappa a - igb + \sqrt{2\kappa}a_{\text{in}}$ and $\dot{b} = -iga$. The input-output relation for the cavity is $a_{\text{out}} = -a_{\text{in}} + \sqrt{2\kappa}a$. We consider the situation where the cavity decay rate $\kappa \gg g$ (and it is also much greater than the bandwidth of the input light). One can then adiabatically eliminate the cavity mode [25,26], $a(t) = (1/\kappa)(-igb + \sqrt{2\kappa}a_{\text{in}})$. This gives the equation of motion $\dot{b} = -Gb - i\sqrt{2G}a_{\text{in}}$ with $G = g^2/\kappa$, and the input-output relation $a_{\text{out}} = a_{\text{in}} - i\sqrt{2G}b$. The solution is $b(t) = -i\sqrt{2G}e^{-Gt} \int_0^t e^{Gt'} a_{\text{in}}(t') dt' + e^{-Gt} b(0)$ for the mechanical mode and $a_{\text{out}}(t) = -i\sqrt{2G}e^{-Gt} b(0) + a_{\text{in}}(t) - 2Ge^{-Gt} \int_0^t e^{Gt'} a_{\text{in}}(t') dt'$ for the output field.

Both storage and retrieval can be implemented by applying a constant coupling strength G for a time duration τ (each). Using techniques similar to those of Ref. [25] one can then show that

$$A_{\text{out}} = -(1-y^2)(A_{\text{in}} + \alpha) - iy\sqrt{1-y^2}B_{\text{in}} + y\delta A, \quad (2)$$

see also the Supplemental Material [22]. Here A_{out} is the optical output mode after storage and retrieval (but before the eventual displacement back to the microscopic level), $y = e^{-G\tau}$, A_{in} is the optical input mode, B_{in} is the initial state of the mechanical oscillator, and δA is an optical noise mode that is in the vacuum state. One can see that the overall storage and retrieval efficiency is $(1-y^2)^2$ (in terms of photon number). This is very similar to the expressions obtained for the efficiency in other types of quantum memories [27].

The displaced two-mode squeezed state is Gaussian. Its entanglement can therefore be quantified via the logarithmic negativity [28]. Expressing Eq. (2) in terms of quadratures one has $X_A^{\text{out}} = -(1-y^2)(X_A^{\text{in}} + \sqrt{2}\alpha) + y\sqrt{1-y^2}P_B^{\text{in}} + y\delta X_A$ and $P_A^{\text{out}} = -(1-y^2)P_A^{\text{in}} - y\sqrt{1-y^2}X_B^{\text{in}} + y\delta P_A$, where X_A^{out} , P_A^{out} , X_B , P_B , δX_A , δP_A are the quadrature operators corresponding to A_{out} , respectively. It is then straightforward to determine the covariance matrix for the output modes and calculate the logarithmic negativity, see also the Supplemental Material [22]. Note that in this calculation the covariance matrix does not depend on the displacement, since α is fixed and mean values are subtracted in the definition of V . This changes, however, in the presence of phase noise, see below. Figure 2 shows the entanglement in the final state as

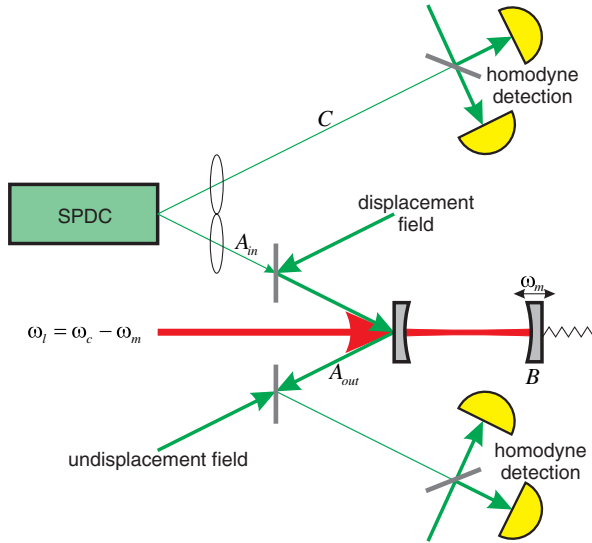


FIG. 1 (color online). Proposed setup. The spontaneous parametric down-conversion source (SPDC) creates a (microscopic) two-mode squeezed state. One mode is directly detected by homodyne detection. The other mode is displaced by a macroscopic amount through the interference with a strong displacement field and then stored onto a mechanical oscillator using an optomechanical cavity and a strong red-detuned control beam. This creates optomechanical micro-macro entanglement. The state of the mechanical system can subsequently be reconverted into light. The entanglement is detected by first displacing the mode back to the microscopic level, followed by homodyne detection.

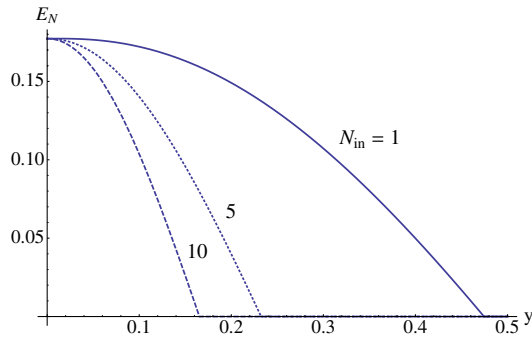


FIG. 2 (color online). Entanglement in the final state as a function of the optomechanical coupling parameter $y = e^{-G\tau}$, for different values of the initial mechanical phonon number N_{in} . In all cases y has to be below a certain threshold value for entanglement to be observable, where the value of the threshold depends on N_{in} . The figure also includes the effect of other imperfections; the relevant parameter values are $x = \gamma/G = 0.01$ and $N_{\text{th}} = 10$ (mechanical noise), $\eta_1 = \eta_2 = \eta_c = 0.8$ (losses), $\sigma = 0.01$ (phase noise); see the text for more discussion. The photon (or phonon) number corresponding to the displacement is $N_D = |\alpha|^2 = 5000$, and the squeezing parameter is $r = 0.5$.

a function of y . One can see that there is a threshold for y above which the entanglement becomes exactly zero. The value of this threshold depends on the initial phonon number $N_{\text{in}} = \langle ((X_B^{\text{in}})^2 + (P_B^{\text{in}})^2 - 1)/2 \rangle$ of the mechanical oscillator. Precooling the mechanical oscillator close to the ground state is helpful for entanglement detection, but not strictly necessary. Note that the red-detuned control beam that is applied in the present protocol has a cooling effect [14]. Figure 2 includes the effects of several other imperfections, namely phase noise, mechanical decoherence, in- and out-coupling loss, and loss on the micro side. We now discuss these effects in more detail.

Phase noise can be modeled through the transformation $A_{\text{out}} \rightarrow e^{i\phi} A_{\text{out}}$, with a random phase ϕ with distribution $p(\phi)$. Let us assume that $p(\phi)$ is symmetric around $\phi = 0$ and has a standard deviation σ , where $\sigma \ll 1$. The only term contributing to the covariance matrix that is significantly affected by the phase noise is $\langle (P_A^{\text{out}})^2 \rangle$, which gets an additional term $2|\alpha|^2(1 - y^2)^2\sigma^2$. All other matrix elements only receive $O(\sigma^2)$ corrections (without the enhancement by the large $|\alpha|^2$ factor). However, this change in $\langle (P_A^{\text{out}})^2 \rangle$, which is not undone by the final displacement back to the microscopic level, has a significant effect on the entanglement, see Fig. 3. Phase noise limits the size of the displacement for which entanglement can be shown. This increasing sensitivity to phase noise for increasing displacement provides further evidence (in addition to the above argument based on the photon or phonon number variances of the displaced Fock states) that the displaced two-mode squeezed state is indeed a macroscopic superposition state, see also Refs. [3,4,6,29,30]. Reference [3] achieved very large displacements ($N_D > 10^8$) by using the

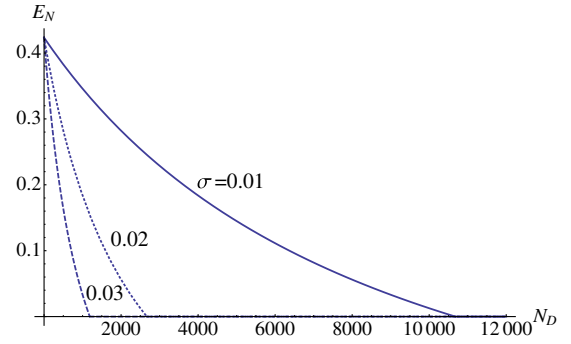


FIG. 3 (color online). Entanglement in the final state as a function of the displaced photon (or phonon) number $N_D = |\alpha|^2$, for different values of the phase noise standard deviation σ . Phase noise limits the size of the displacement for which entanglement can be shown. Here $y = 0.1$, $N_{\text{in}} = 1$, and the other parameters are the same as in Fig. 2.

same spatial mode (but orthogonal polarization modes) for the signal and displacement beam, leading to very high stability. This may be more challenging in the optomechanical context. In our examples we have picked σ values more comparable to Ref. [4], where the signal and displacement beam were in separate spatial modes.

We will now take into account the mechanical damping and associated noise. The equation of motion for b is now $\dot{b} = -\gamma b - iga + \sqrt{2\gamma}b_{\text{in}}$, leading to $\dot{b} = -G'b - i\sqrt{2G}a_{\text{in}} + \sqrt{2\gamma}b_{\text{in}}$ after adiabatic elimination of the cavity mode. Here $G' = G + \gamma$. Using techniques similar to Ref. [25], but keeping all orders of γ , one can show that this equation together with the input-output relation for the cavity leads to the following modified equation for the optical output mode after storage and retrieval:

$$A_{\text{out}} = -\frac{1 - y^2}{1 + x} A_{\text{in}} - i\sqrt{\frac{1 - y^2}{1 + x}} y B_{\text{in}} + f_1 \delta A + f_2 \delta B,$$

where we have introduced the notation $x = \gamma/G$, and A_{in} is defined analogously to before, but using G' instead of G . The modes δA and δB correspond to the optical and mechanical noise, respectively, where the former is in the vacuum state, and the latter is in a thermal state at the temperature of the mechanical bath with a mean phonon number N_{th} . The expressions for the coefficients f_1 and f_2 , as well as more details on the calculation, are given in the Supplemental Material [22]. Figure 4 shows the effect of the mechanical noise on the entanglement in the final state; x has to be below a certain threshold in order for entanglement to be present, where the value of the threshold depends on N_{th} . For the parameters of Fig. 4 one has the condition $N_{\text{th}}x = N_{\text{th}}\gamma/G \lesssim 0.2$; $N_{\text{th}}\gamma$ can be interpreted as the effective mechanical decoherence rate.

Another important imperfection is photon loss, including coupling losses for the optomechanical cavity and detection inefficiency. These effects are discussed in the

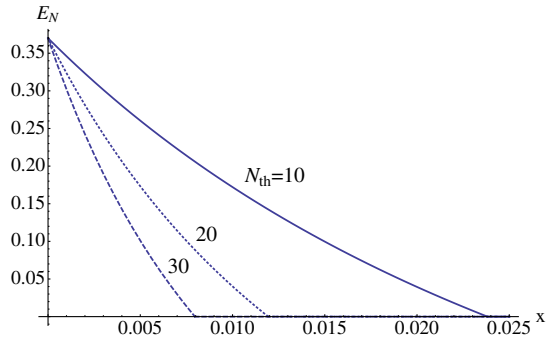


FIG. 4 (color online). Entanglement in the final state as a function of the mechanical noise parameter $x = \gamma/G$, for different values of the bath mean phonon number N_{th} . The values of the other parameters are $N_D = |\alpha|^2 = 5000$, $r = 0.5$, $y = 0.1$, $N_{\text{in}} = 1$, $\sigma = 0.01$, and $\eta_1 = \eta_2 = \eta_c = 0.8$.

Supplemental Material [22]. Most importantly, Fig. 2 of the Supplemental Material [22] shows that the cavity in-coupling efficiency has to be above a certain threshold value (of order 0.4 for our choice of parameters) in order to be able to demonstrate entanglement.

We propose an implementation based on the integrated optical and mechanical nanoscale resonator of Ref. [14] and the narrow band cavity-enhanced parametric down-conversion source of Ref. [31]. Taking $\omega_m = 2\pi \times 3.7$ GHz, $\kappa = 2\pi \times 500$ MHz, and $\gamma = 2\pi \times 35$ kHz from Ref. [14] and assuming a bath temperature $T = 2$ K, which is accessible with fairly simple cryostats, one has $N_{\text{th}} \approx 10$. The highest drive power used in Ref. [14] corresponds to $g \approx 2\pi \times 40$ MHz, leading to an effective coupling $G = g^2/\kappa \approx 2\pi \times 3.2$ MHz. This gives $x = \gamma/G \approx 0.01$. We propose $\tau \approx 100$ ns, which is in good correspondence with Ref. [31]. This gives $y = e^{-G\tau} \approx 0.1$. Concerning photon loss, Ref. [32] already demonstrated of order 75% in-coupling efficiency and 52% out-coupling efficiency, and even higher values should be possible. We have neglected the effects of the squeezing part of the optomechanical Hamiltonian. They are expected to be suppressed by a factor $(\kappa/\omega_m)^2$, which is less than 0.02 for the system parameters given above, justifying the approximation for this proposed implementation. Beam-splitter type optomechanical coupling was also demonstrated, e.g., in Refs. [11,19]. The creation and detection of optomechanical micro-macro entanglement is thus within reach of current technology.

The approach based on optomechanical storage and retrieval also allows one to conceive experiments that would test proposals for quantum gravity induced wave function collapse. For example, using the approach of Ref. [33] it is realistic to fabricate trampoline resonators with an effective mass of 500 ng, a mechanical frequency $\omega_m = 2\pi \times 10$ kHz, and a mechanical quality factor of 10^6 . At a temperature of 1 mK the environmentally induced decoherence time scale $1/N_{\text{th}}\gamma$ of 7.6 ms is then

significantly longer than the decoherence times predicted for this system by the quantum gravity induced collapse models of Ref. [34] (240 μ s) and of Ref. [35] (95 μ s), see also Ref. [36]. The latter number is obtained using the nuclear radius to define the mass distribution following Ref. [37]. For a cavity length of 10 cm, a cavity finesse of 10^6 , and a control field power of 40 pW one can then have $\kappa \approx 2\pi \times 1.5$ kHz and $G \approx 2\pi \times 200$ Hz, satisfying $\omega_m \gg \kappa \gg G \gg \gamma N_{\text{th}} \approx 2\pi \times 20$ Hz, as required for side-band cooling, adiabatic elimination of the cavity, and entanglement detection, respectively. These parameters require a source of sub-kHz bandwidth two-mode squeezed light, which should be feasible based on parametric down conversion with a narrow band pump laser in combination with filter cavities. Compared to the proposal of Ref. [17], which may also allow testing collapse models with weakly coupled optomechanical systems, the present approach has the advantage of not requiring any postselection.

While the above-mentioned collapse times are not sensitive to the size of the displacement α , varying α and hence the number of phonons involved in the superposition would also allow one to look for other types of deviations from quantum physics that might manifest in the little explored regime of superpositions of macroscopically different quantum numbers.

This work was supported by AITF, NSERC, NSF Grant No. PHY-1206118, and NWO VICI Grant No. 680-47-604. We thank P. Barclay for useful discussions.

Note added.—In the recently published experiment of Ref. [38] optomechanical entanglement in the microwave domain (created via blue-detuned driving, not by storing an entangled signal) is also detected by mapping the state of the mechanical mode onto the microwave field.

*Present address: Institute of Atomic and Subatomic Physics, TU Wien, Stadionallee 2, 1020 Wien, Austria.

- [1] C. Monroe, D. M. Meekhof, B. E. King, and D. J. Wineland, *Science* **272**, 1131 (1996); M. Arndt, O. Nairz, J. Vos-Andreae, C. Keller, G. van der Zouw, and A. Zeilinger, *Nature (London)* **401**, 680 (1999); J. R. Friedman, V. Patel, W. Chen, S. K. Tolpygo, and J. E. Lukens, *Nature (London)* **406**, 43 (2000); B. Julsgaard, A. Kozhkin, and E. S. Polzik, *Nature (London)* **413**, 400 (2001); S. Deléglise, I. Dotsenko, C. Sayrin, J. Bernu, M. Brune, J.-M. Raimond, and S. Haroche, *Nature (London)* **455**, 510 (2008); R. Fickler, R. Lapkiewicz, W. N. Plick, M. Krenn, C. Schaeff, S. Ramelow, and A. Zeilinger, *Science* **338**, 640 (2012).
- [2] M. Neeley, M. Ansmann, R. C. Bialczak, M. Hofheinz, N. Katz, E. Lucero, A. O'Connell, H. Wang, A. N. Cleland, and J. M. Martinis, *Nat. Phys.* **4**, 523 (2008); A. D. O'Connell *et al.*, *Nature (London)* **464**, 697 (2010).
- [3] A. I. Lvovsky, R. Ghobadi, A. Chandra, A. S. Prasad, and C. Simon, *Nat. Phys.* **9**, 541 (2013).
- [4] N. Bruno, A. Martin, P. Sekatski, N. Sangouard, R. T. Thew, and N. Gisin, *Nat. Phys.* **9**, 545 (2013).

- [5] S. Raeisi, W. Tittel, and C. Simon, *Phys. Rev. Lett.* **108**, 120404 (2012).
- [6] P. Sekatski, N. Sangouard, M. Stobińska, F. Bussières, M. Afzelius, and N. Gisin, *Phys. Rev. A* **86**, 060301(R) (2012).
- [7] F. De Martini, F. Sciarrino, and C. Vitelli, *Phys. Rev. Lett.* **100**, 253601 (2008).
- [8] R. Ghobadi, A. I. Lvovsky, and C. Simon, *Phys. Rev. Lett.* **110**, 170406 (2013).
- [9] F. De Martini, F. Sciarrino, C. Vitelli, and F. S. Cataliotti, *Phys. Rev. Lett.* **104**, 050403 (2010).
- [10] E. Schrödinger, *Naturwissenschaften* **23**, 823 (1935).
- [11] E. Verhagen, S. Deléglise, S. Weis, A. Schliesser, and T. J. Kippenberg, *Nature (London)* **482**, 63 (2012).
- [12] A. H. Safavi-Naeini et al., *Nature (London)* **500**, 185 (2013); T. P. Purdy, R. W. Peterson, and C. Regal, *Science* **339**, 801 (2013); T. P. Purdy, P.-L. Yu, R. W. Peterson, N. S. Kampel, and C. A. Regal, *Phys. Rev. X* **3**, 031012 (2013); J. D. Teufel, T. Donner, D. Li, J. W. Harlow, M. S. Allman, K. Cicak, A. J. Sirois, J. D. Whittaker, K. W. Lehnert, and R. W. Simmonds, *Nature (London)* **475**, 359 (2011).
- [13] M. Aspelmeyer, T. J. Kippenberg, and F. Marquardt, *arXiv:1303.0733*.
- [14] J. Chan, T. P. Mayer Alegre, A. H. Safavi-Naeini, J. T. Hill, A. Krause, S. Gröblacher, M. Aspelmeyer, and O. Painter, *Nature (London)* **478**, 89 (2011).
- [15] W. Marshall, C. Simon, R. Penrose, and D. Bouwmeester, *Phys. Rev. Lett.* **91**, 130401 (2003).
- [16] O. Romero-Isart, M. L. Juan, R. Quidant, and J. I. Cirac, *New J. Phys.* **12**, 033015 (2010).
- [17] B. Pepper, R. Ghobadi, E. Jeffrey, C. Simon, and D. Bouwmeester, *Phys. Rev. Lett.* **109**, 023601 (2012).
- [18] V. Fiore, Y. Yang, M. C. Kuzyk, R. Barbour, L. Tian, and H. Wang, *Phys. Rev. Lett.* **107**, 133601 (2011).
- [19] T. A. Palomaki, J. W. Harlow, J. D. Teufel, R. W. Simmonds, and K. W. Lehnert, *Nature (London)* **495**, 210 (2013).
- [20] O. Romero-Isart, A. C. Pflanzner, F. Blaser, R. Kaltenbaek, N. Kiesel, M. Aspelmeyer, and J. I. Cirac, *Phys. Rev. Lett.* **107**, 020405 (2011); Z. Q. Yin, T. Li, X. Zhang, and L. M. Duan, *Phys. Rev. A* **88**, 033614 (2013).
- [21] S. Raeisi, P. Sekatski, and C. Simon, *Phys. Rev. Lett.* **107**, 250401 (2011).
- [22] See Supplemental Material at <http://link.aps.org/supplemental/10.1103/PhysRevLett.112.080503> for a discussion of displaced single-photon entanglement and for more details on several calculations mentioned in the text.
- [23] M. G. A. Paris, *Phys. Lett. A* **217**, 78 (1996); G. M. D'Ariano and M. F. Sacchi, *Phys. Rev. A* **52**, R4309 (1995).
- [24] A. I. Lvovsky and S. A. Babichev, *Phys. Rev. A* **66**, 011801 (R) (2002).
- [25] S. G. Hofer, W. Wiecek, M. Aspelmeyer, and K. Hammerer, *Phys. Rev. A* **84**, 052327 (2011).
- [26] J. Zhang, K. Peng, and S. L. Braunstein, *Phys. Rev. A* **68**, 013808 (2003).
- [27] See, e.g., Sec. 6 of C. Simon *et al.*, *Eur. Phys. J. D* **58**, 1 (2010); K. Heshami, A. Green, Y. Han, A. Rispe, E. Saglamyurek, N. Sinclair, W. Tittel, and C. Simon, *Phys. Rev. A* **86**, 013813 (2012).
- [28] G. Adesso, A. Serafini, and F. Illuminati, *Phys. Rev. A* **70**, 022318 (2004).
- [29] W. Dür, C. Simon, and J. I. Cirac, *Phys. Rev. Lett.* **89**, 210402 (2002).
- [30] P. Sekatski, N. Sangouard, N. Gisin, and *arXiv:1306.0843*.
- [31] J. Fekete, D. Rieländer, M. Cristiani, and H. de Riedmatten, *Phys. Rev. Lett.* **110**, 220502 (2013).
- [32] J. D. Cohen, S. M. Meenehan, and O. Painter, *Opt. Express* **21**, 11227 (2013).
- [33] D. Kleckner, B. Pepper, E. Jeffrey, P. Sonin, S. M. Thon, and D. Bouwmeester, *Opt. Express* **19**, 19708 (2011).
- [34] J. Ellis, J. S. Hagelin, D. V. Nanopoulos, and M. Srednicki, *Nucl. Phys.* **B241**, 381 (1984); J. Ellis, S. Mohanty, and D. V. Nanopoulos, *Phys. Lett. B* **221**, 113 (1989).
- [35] L. Diósi, *Phys. Rev. A* **40**, 1165 (1989); R. Penrose, *Gen. Relativ. Gravit.* **28**, 581 (1996).
- [36] B. Collett and P. Pearle, *Found. Phys.* **33**, 1495 (2003); D. Kleckner, I. Pikovski, E. Jeffrey, L. Ament, E. Eliel, J. van den Brink, and D. Bouwmeester, *New J. Phys.* **10**, 095020 (2008); O. Romero-Isart, *Phys. Rev. A* **84**, 052121 (2011); B. Pepper, E. Jeffrey, R. Ghobadi, C. Simon, and D. Bouwmeester, *New J. Phys.* **14**, 115025 (2012).
- [37] L. Diósi, *J. Phys. A* **40**, 2989 (2007).
- [38] T. A. Palomaki, J. D. Teufel, R. W. Simmonds, and K. W. Lehnert, *Science* **342**, 710 (2013).